

Saliency-Based Change Detection for Aerial and Remote Sensing Imageries

Hui Li Tan, Shijian Lu

Institute for Infocomm Research (I²R), A*STAR, Singapore

{hltan, slu}@i2r.a-star.edu.sg

Abstract—Change detection for aerial and remote sensing imageries is an important research topic with a wide range of applications in urban and environmental studies, emergency management, etc. It is a challenging problem due to various types of acquisition or environmental noises in the captured images. In this paper, we propose a saliency-based change detection technique that makes use of two-dimensional within-images and between-images co-occurrence histogram saliency. Our experimental results show that the proposed method can effectively detect true changes of semantic interest while suppressing false changes due to acquisition or environmental noises.

I. INTRODUCTION

Unmanned systems have seen unprecedented levels of growth in the last decade. Equipped with more advanced reconnaissance and surveillance capabilities, unmanned systems today play greater roles in a wide range of applications including ecosystem monitoring and planning, land use monitoring and planning, disaster assessment, humanitarian relief, etc.

Change detection for the aerial and remote sensing imageries seeks to detect changes between two images of the same geographical area at different times. It is a challenging problem as not all physical changes are semantically useful. As the images are taken at different times, there could be additional atmospheric condition changes, illumination changes, registration changes, etc. Furthermore, if the images are taken at a long period of time apart, there could also be additional seasonal changes such as browning of vegetation, shedding of vegetation, and covering of snow. These additional changes make it difficult to detect semantically useful changes such as construction of or modification to structures, mass changes to ecosystem and land use, etc.

Aerial and remote sensing based change detection is an active research topic, and has been applied to a broad range of data products including grayscale, color, multispectral, hyperspectral and synthetic aperture radar imagery. Reviews are provided by Mas et al. [1] and Singh et al. [2]. Producing the difference images and binary classifying the difference images are two key procedures.

The most common way to produce the difference images is the image subtraction method [2] in which a subtraction image is obtained from two images, where the two images could be the aerial or remote sensing images, vegetation indexes, or principal components derived from the aerial or remote sensing images. In the univariate image differencing method, the difference image is obtained from a single spectral band decided by the type of change to be detected. In the

change vector analysis (CVA) method, the difference image is obtained from several spectral bands. Another common way is the image rationing method [2] in which a ratio image is obtained from two images. Various improvements such as the mean-filtered subtraction [3], log-ratio [4], and mean-ratio [4] have also been explored. Other difference measures, such as change field [5] using SIFT [6] or Daisy [7] features, have also been investigated.

Given the difference images, binary classification can be performed to obtain the final changed and unchanged regions. Supervised methods [8], [9], [10], semi-supervised methods, and unsupervised methods [11], [12], [13] can be used to achieve the binary classification. The supervised methods are generally robust to different acquisition and environmental conditions, but can be limited in application and degree of automation due to the need of ground truth information. On the other hand, the unsupervised methods do not require additional ground truth information, and are thus widely used.

Since physical changes may not always be semantically useful, recent works explored the use of visual saliency for change detection. Tian et al. and Wang et al. explored saliency-based change detection for multispectral images. Tian et al. used a modified Itti visual saliency model [14] on the difference images of multi-features for change detection [15]. Wang et al. applied a modified spectral residual error and phase spectrum information saliency algorithm to the difference images to select regions with high saliency, and then applied a modified fuzzy clustering method to the salient difference images to obtain the final changed and unchanged regions [16]. Furthermore, Zheng et al. and Wang et al. explored saliency-based change detection for synthetic aperture radar images. Zheng et al. used an unsupervised approach [17], whereby the context-aware saliency method [18] was applied to the log ratio difference images to extract the regions of interest, and then the principal component analysis (PCA) and k-means clustering was applied to obtain the final changed and unchanged regions. Wang et al. used a semi-supervised Laplacian support vector machine (SVM) [19], whereby the context-aware saliency method [18] was applied to generate a pseudo-training set to initialize the SVM.

Since existing saliency modelling methods are designed for single image, prior saliency-based change detection methods leverage on existing saliency modelling methods by directly applying the saliency modelling to the single difference image derived from the two source images. In this paper, we propose

a saliency-based change detection algorithm that is capable of detecting true changes of semantic interest while suppressing false changes due to acquisition or environmental conditions as shown in Fig. 1. Our proposed approach directly utilize the two source images to capture within-images and between-images saliency.

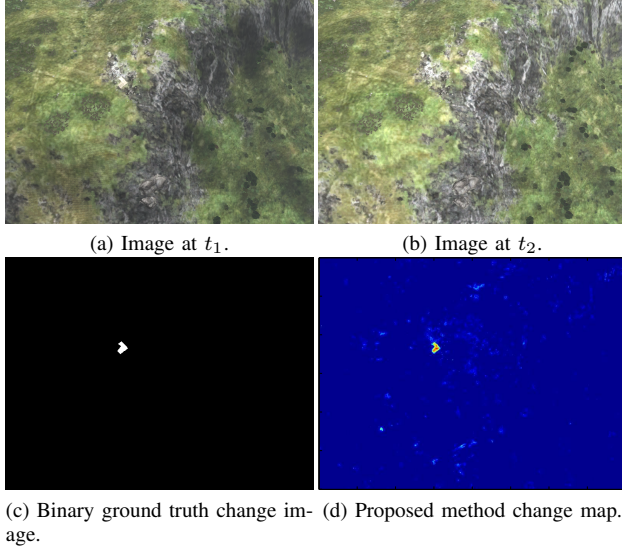


Fig. 1: Proposed technique on change detection for aerial and remote sensing imageries.

II. PROPOSED METHOD

We propose a saliency-based change detection algorithm that makes use of two-dimensional (2D) within-images and between-images co-occurrence histogram saliency.

Let I_1 and I_2 denote two images of the same geographical area at different times. Then, 2D within-images co-occurrence histograms [20], $H_{(1,1)}$ and $H_{(2,2)}$, and 2D between-images co-occurrence histograms, $H_{(1,2)}$ and $H_{(2,1)}$, are constructed as:

$$H_{(t_a,t_b)}(m, n) = \sum_{I_{t_a}(i,j)=m} \sum_{i'=i-z}^{i+z} \sum_{j'=j-z}^{j+z} \begin{cases} 1, & \text{if } I_{t_b}(i', j') = n \\ 0, & \text{if otherwise} \end{cases}. \quad (1)$$

Coordinate (i, j) denotes a pixel position in image I_{t_a} , while coordinate (i', j') denotes a pixel position in image I_{t_b} . Furthermore, coordinate (m, n) , where $m \in D, n \in D$, denotes a position in the 2D co-occurrence histogram. D denotes the possible values in images I_{t_a} and I_{t_b} , i.e., the dynamic range of images I_{t_a} and I_{t_b} . Variables $(t_a, t_b) = \{(1,1), (2,2), (1,2), (2,1)\}$, and z denotes a neighbourhood size which is experimentally set as two.

In other words, for each pixel in image I_{t_a} with image value m , the occurrence of neighbouring pixels in image I_{t_b} with image value n contributes to the 2D co-occurrence histogram count $H_{(t_a,t_b)}(m, n)$. Visual saliency is often perceived by global rarity and local discontinuity with respect to its local neighbourhood. Therefore, by concurrently encoding both

global pixel occurrences and local co-occurrences of pixel pairs within a neighbourhood window, the 2D co-occurrence histogram captures both global and local saliency information.

When $I_{t_a} = I_{t_b}$, as in [20], the 2D co-occurrence histograms are computed from a single image to give within-images histograms. Therefore, $H_{(1,1)}$ and $H_{(2,2)}$ model the 2D within-images occurrence and co-occurrence patterns. On the other hand, when $I_{t_a} \neq I_{t_b}$, an extension of the co-occurrence histogram concept for image pairs, the 2D co-occurrence histograms are computed across two images to give between-images histograms. Therefore, $H_{(1,2)}$ and $H_{(2,1)}$ model the 2D between-images occurrence and co-occurrence patterns.

Since saliency is negatively correlated with occurrence and co-occurrence patterns, inverted distribution functions, $P_{(1,2)}$, $P_{(2,1)}$, $P_{(1,1)}$, $P_{(2,2)}$, are computed as:

$$P_{(t_a,t_b)}(m, n) = \begin{cases} \frac{1}{\|H_{(t_a,t_b)}\|_0} - \frac{H_{(t_a,t_b)}(m,n)}{\sum_{\forall m} \sum_{\forall n} H_{(t_a,t_b)}(m,n)}, \\ \text{if } \frac{1}{\|H_{(t_a,t_b)}\|_0} - \frac{H_{(t_a,t_b)}(m,n)}{\sum_{\forall m} \sum_{\forall n} H_{(t_a,t_b)}(m,n)} \geq 0 \\ 0, \\ \text{if otherwise} \end{cases}, \quad (2)$$

where $\|H_{(t_a,t_b)}\|_0$ is the number of non-zero elements in $H_{(t_a,t_b)}$. The threshold ensures that image value pairs that are more common than average are not considered salient.

Subsequently, 2D between-images co-occurrence histogram saliency maps, $S_{(1,2)}$ and $S_{(2,1)}$, and within-images co-occurrence histogram saliency maps, $S_{(1,1)}$ and $S_{(2,2)}$, are constructed as:

$$S_{(t_a,t_b)}(i, j) = \sum_{i'=i-z}^{i+z} \sum_{j'=j-z}^{j+z} P_{(t_a,t_b)}(I_{t_a}(i, j), I_{t_b}(i', j')). \quad (3)$$

The process of constructing 2D within-images and between-images co-occurrence histogram saliency maps for a single channel image is illustrated in Fig. 2. The saliency maps for a multiple channel image are obtained by maximum operation.

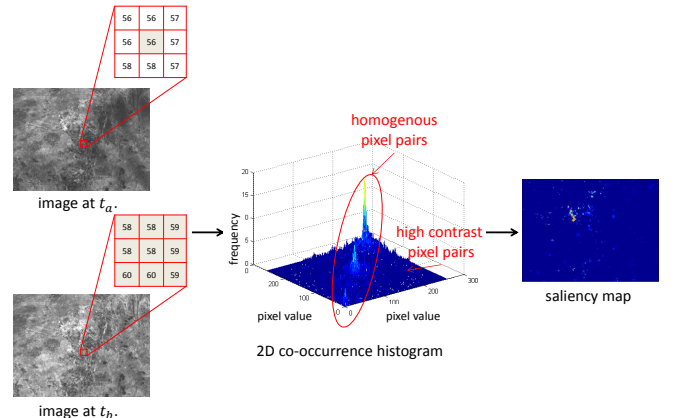


Fig. 2: Process of constructing 2D within-images and between-images co-occurrence histogram saliency maps.

As shown in Fig. 3, based on the image pair in Fig. 1(a) and Fig. 1(b), the between-images saliency maps, $S_{(1,2)}$ and $S_{(2,1)}$, clearly capture the salient changes between images I_{t_a} and I_{t_b} . On the other hand, the within-images saliency maps $S_{(1,1)}$ and $S_{(2,2)}$, clearly capture the salient regions within image I_{t_a} and within image I_{t_b} respectively.

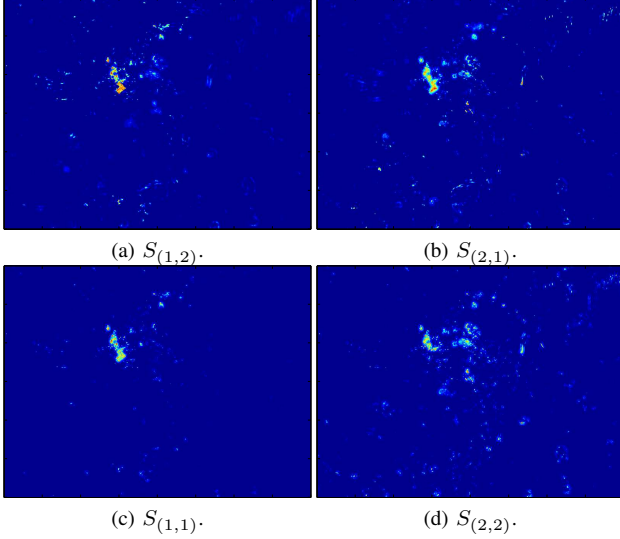


Fig. 3: Between-images and within-images co-occurrence histogram saliency maps.

By utilizing the 2D between-images and within-images saliency maps, the final saliency map is constructed as:

$$\begin{aligned} & S(i,j) \\ &= |S_{(1,2)}(i,j) + S_{(2,1)}(i,j) - S_{(2,2)}(i,j) - S_{(1,1)}(i,j)|. \end{aligned} \quad (4)$$

The within-images saliency maps normalize the cases where the between-images saliency maps are high due to high within-images saliency.

III. EXPERIMENTAL RESULTS

We evaluated our proposed saliency-based change detection method on the publicly available aerial imagery change detection (AICD) dataset [21]. The AICD dataset includes 100 different scenes, where a reference image, a test image, and a corresponding ground truth mask of significant change are provided for each scene. As illustrated in the first two rows of Fig. 4, the reference and test images differ in the absence/presence of one significant change as well as the direction of sunlight giving illumination changes and shadows. The proposed method was compared against the change vector analysis (CVA) [2], SIFT feature analysis [6], Daisy features analysis [7], Itti visual saliency model [14] on difference image (IKN-diff), and context-aware saliency detection algorithm [18] on log ratio difference image (CAS-diff).

Examples from the AICD dataset are shown in Figure 4. It can be seen that, in the presence of both strong and mild illumination changes and shadows, the proposed method can clearly identify the semantically useful changes. Thus, the proposed method provides a more effective way to cull

through huge volume of aerial and remote sensing imageries and narrow down the scope that human analysts would need to manually examine.

Examples 1 and 2 illustrate the case of strong illumination changes. In the difference images (CVA change maps) derived from the source images, true changes of little intensity changes can be masked by false changes of large intensity changes, even when an object of interest is salient. By applying saliency modelling to such difference images, true changes of little intensity changes are extracted with false changes of large intensity changes. On the other hand, for the proposed method, the 2D between-images co-occurrence histogram captures the actual illumination mapping between the source images, and thus models such illumination changes as not so salient.

Examples 4 and 5 illustrate the case of shadow changes. The presence of shadows around objects above ground also often lead to large intensity changes which are captured on the difference maps. By applying saliency modelling to such difference images, true changes may be extracted as equally salient as such shadow changes. For the proposed method, the 2D between-images co-occurrence histogram captures the shadow to non-shadow or non-shadow to shadow mapping between the source images, and thus models such shadow changes as not so salient.

All change maps were processed using the Otsu's thresholding algorithm [22] to obtain the final changed and unchanged regions. The average accuracies over the dataset (%) obtained by the various methods are shown in Table I. The accuracy is defined as the total number of true positives and true negatives over the total number of pixels in the image.

Method	Accuracy (%)
CVA	73.60
SIFT feature analysis	52.28
Daisy feature analysis	84.32
IKN-diff	93.36
CAS-diff	91.05
Proposed	98.72

TABLE I: Average accuracies over AICD dataset (%).

In general, the saliency-based methods obtained higher accuracies. This is mainly contributed by much lower false alarms, due to the abilities of the saliency-based methods to suppress non-significant changes due to illumination and shadow, and highlight significant changes to ecosystem or land use. Furthermore, the proposed method obtained the highest accuracy, suggesting the effectiveness of the proposed method.

IV. CONCLUSION

In this paper, we have proposed a saliency-based change detection technique that makes use of 2D between-images and within-images co-occurrence histogram saliency. Experimental results have shown that the proposed method can effectively detect true changes of interest while suppressing false changes due to acquisition or environmental conditions. Our future research includes extending the change detection algorithm to better handle larger mis-registration changes due to larger view angle variations.

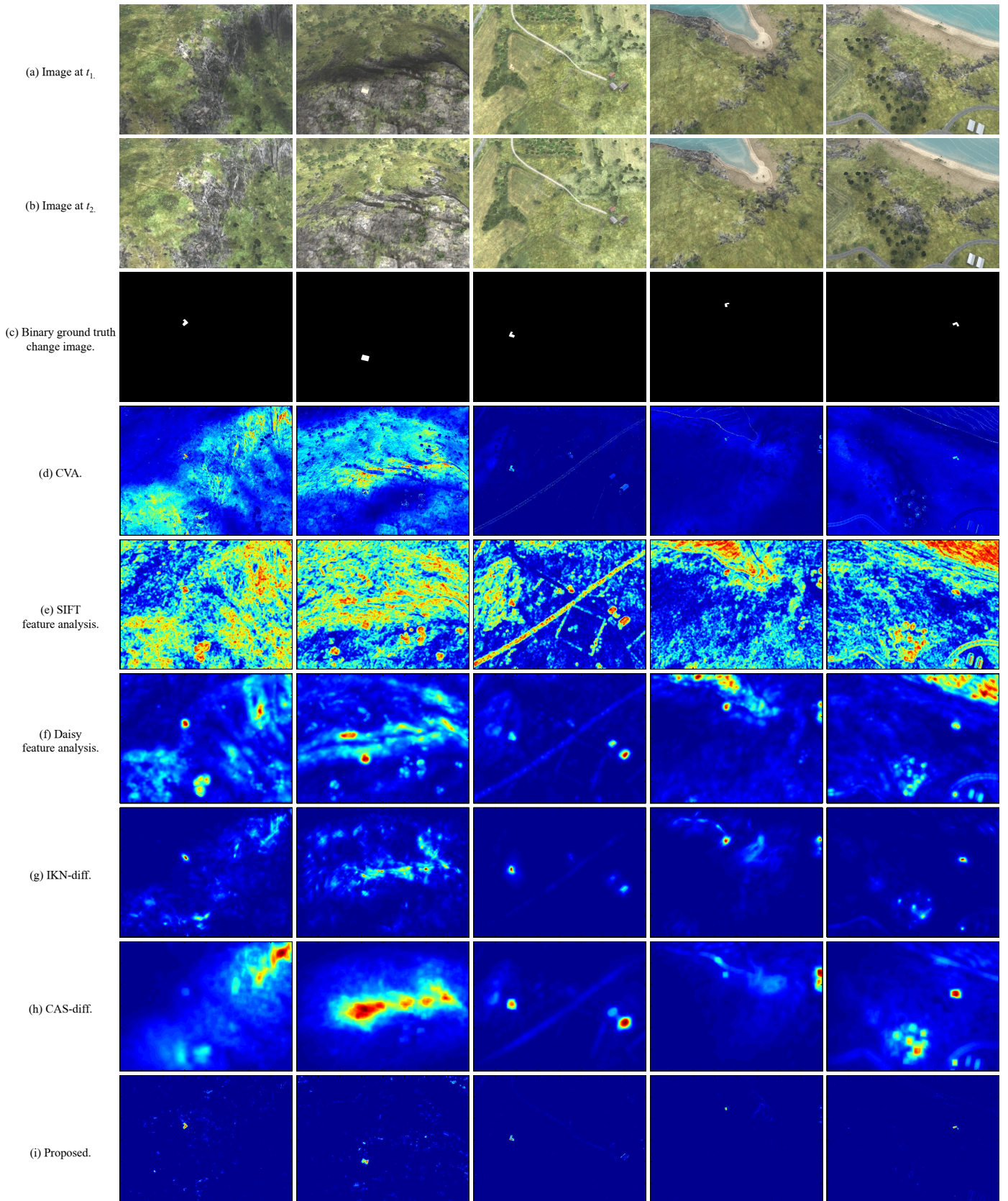


Fig. 4: Examples from the AICD dataset to illustrate the performances of various change detection methods in the presence of illumination changes and shadows.

REFERENCES

- [1] J.-F. Mas, "Monitoring land-cover changes: A comparison of change detection techniques," *International Journal of Remote Sensing*, vol. 20, no. 1, pp. 139–152, 1999. [Online]. Available: <http://dx.doi.org/10.1080/014311699213659>
- [2] A. Singh, "Review article digital change detection techniques using remotely-sensed data," *International Journal of Remote Sensing*, vol. 10, no. 6, pp. 989–1003, 1989. [Online]. Available: <http://dx.doi.org/10.1080/01431168908903939>
- [3] Y. Zheng, X. Zhang, B. Hou, and G. Liu, "Using combined difference image and k-means clustering for SAR image change detection," *IEEE Geoscience and Remote Sensing Letters*, vol. 11, no. 3, pp. 691–695, Mar 2014.
- [4] M. Gong, Z. Zhou, and J. Ma, "Change detection in synthetic aperture radar images based on image fusion and fuzzy clustering," *IEEE Transactions on Image Processing*, vol. 21, no. 4, pp. 2141–2151, Apr 2012.
- [5] L. Huo, X. Feng, C. Huo, Z. Zhou, and C. Pan, "Change field: A new change measure for VHR images," *IEEE Geoscience and Remote Sensing Letters*, vol. 11, no. 10, pp. 1812–1816, Oct 2014.
- [6] D. G. Lowe, "Distinctive image features from scale-invariant keypoints," *Int. J. Comput. Vision*, vol. 60, no. 2, pp. 91–110, Nov. 2004. [Online]. Available: <http://dx.doi.org/10.1023/B:VISI.0000029664.99615.94>
- [7] E. Tola, V. Lepetit, and P. Fua, "A fast local descriptor for dense matching," in *Proceedings of Computer Vision and Pattern Recognition*, Alaska, USA, 2008.
- [8] G. Cao, Y. Li, Y. Liu, and Y. Shang, "Automatic change detection in high-resolution remote-sensing images by means of level set evolution and support vector machine classification," *International Journal of Remote Sensing*, vol. 35, no. 16, pp. 6255–6270, 2014. [Online]. Available: <http://dx.doi.org/10.1080/01431161.2014.951740>
- [9] B. Demir, F. Bovolo, and L. Bruzzone, "Detection of land-cover transitions in multitemporal remote sensing images with active-learning-based compound classification," *IEEE Transactions on Geoscience and Remote Sensing*, vol. 50, no. 5, pp. 1930–1941, May 2012.
- [10] X. Li, Y. Zhang, X. Liu, and Y. Chen, "Assimilating process context information of cellular automata into change detection for monitoring land use changes," *International Journal of Geographical Information Science*, vol. 26, no. 9, pp. 1667–1687, 2012. [Online]. Available: <http://dx.doi.org/10.1080/13658816.2011.643803>
- [11] S. Patra, S. Ghosh, and A. Ghosh, "Histogram thresholding for unsupervised change detection of remote sensing images," *International Journal of Remote Sensing*, vol. 32, no. 21, pp. 6071–6089, 2011. [Online]. Available: <http://dx.doi.org/10.1080/01431161.2010.507793>
- [12] M. Hao, H. Zhang, W. Shi, and K. Deng, "Unsupervised change detection using fuzzy c-means and MRF from remotely sensed images," *Remote Sensing Letters*, vol. 4, no. 12, pp. 1185–1194, 2013. [Online]. Available: <http://dx.doi.org/10.1080/2150704X.2013.858841>
- [13] Y. Bazi, F. Melgani, and H. D. Al-Sharari, "Unsupervised change detection in multispectral remotely sensed imagery with level set methods," *IEEE Transactions on Geoscience and Remote Sensing*, vol. 48, no. 8, pp. 3178–3187, Aug 2010.
- [14] L. Itti, C. Koch, and E. Niebur, "A model of saliency-based visual attention for rapid scene analysis," *IEEE Transactions on Pattern Analysis and Machine Intelligence*, vol. 20, no. 11, pp. 1254–1259, Nov 1998.
- [15] M. Tian, S. Wan, and L. Yue, "A novel approach for change detection in remote sensing image based on saliency map," in *Computer Graphics, Imaging and Visualisation (CGIV 2007)*, Aug 2007, pp. 397–402.
- [16] Q. Wang and X. Zhang, "A novel visual saliency guided high resolution remote sensing image change detection algorithm," *International Conference on Computer Sciences and Automation Engineering (ICCSAE)*, 2015.
- [17] Y. Zheng, L. Jiao, H. Liu, X. Zhang, B. Hou, and S. Wang, "Unsupervised saliency-guided SAR image change detection," *Pattern Recognition*, vol. 61, pp. 309–326, 2017. [Online]. Available: <http://www.sciencedirect.com/science/article/pii/S0031320316301984>
- [18] S. Goferman, L. Zelnik-Manor, and A. Tal, "Context-aware saliency detection," *IEEE Transactions on Pattern Analysis and Machine Intelligence*, vol. 34, no. 10, pp. 1915–1926, Oct 2012.
- [19] S. Wang, S. Yang, and L. Jiao, "Saliency-guided change detection for SAR imagery using a semi-supervised laplacian svm," *Remote Sensing Letters*, vol. 7, no. 11, pp. 1043–1052, 2016. [Online]. Available: <http://dx.doi.org/10.1080/2150704X.2016.1212417>
- [20] S. Lu, C. Tan, and J. H. Lim, "Robust and efficient saliency modeling from image co-occurrence histograms," *IEEE Transactions on Pattern Analysis and Machine Intelligence*, vol. 36, no. 1, pp. 195–201, Jan 2014.
- [21] N. Bourdis, D. Marraud, and H. Sahbi. Change detection dataset. [Online]. Available: <http://www.computervisiononline.com/dataset/1105138664>
- [22] N. Otsu, "A threshold selection method from gray-level histograms," *IEEE Transactions on Systems, Man and Cybernetics*, vol. 9, no. 1, pp. 62–66, Jan. 1979. [Online]. Available: <http://dx.doi.org/10.1109/tsmc.1979.4310076>